Catalytic Mismatching of $CuInSe_2$ and Ni_3Al Demonstrates Selective Photoelectrochemical CO_2 Reduction to Methanol

Brian M. Foster, Aubrey R. Paris, Jessica J. Frick, Daniel A. Blasini-Pérez, Robert J. Cava, Andrew B. Bocarsly*

Department of Chemistry, Princeton University, Princeton, New Jersey, USA 08544

KEYWORDS: CO_2 reduction, photoelectrochemistry, Ni_3Al, $CuInSe_2$, chalcogenides, methanol

Supporting Information Placeholder

ABSTRACT: Photoelectrochemical catalysts are often plagued by ineffective interfacial charge-transfer or nonideal optical conversion properties. To overcome this challenge, strategically pairing a catalytically inactive, optically proficient semiconductor with a selective electrocatalyst—coined "catalytic mismatching"—is suggested. Here, chalcopyrite semiconductor $CuInSe_2$ is paired with the electrocatalyst Ni_3Al to selectively reduce CO_2. This catalytically mismatched system produces methanol at a Faradaic efficiency 25 times greater than that achieved using the purely electrochemical Ni_3Al system while reducing the operating potential requirement by 600 mV. These results suggest that catalytic mismatching is a promising tactic to achieve reaction selectivity in synergistic photoelectrochemical CO_2 reduction systems.

The semiconductor-electrolyte junction offers the opportunity to directly convert optical energy to electrical energy while simultaneously electrocatalyzing a molecular transformation. However, apart from formative work on binary oxide systems,[1,2] finding a material that is efficient at both optical conversion (i.e., at wavelengths of utility for solar photochemistry) and carrying out the selective electrochemical transformation of interest has proven challenging. This goal is further complicated by the fact that most photoelectrochemical interfaces undergo deleterious photodecomposition under illumination, leading to dissolution of the semiconductor material.[3–6]

Design of an operational semiconductor-electrolyte interface is further limited by the fact that an ideal interface only produces electrons at one potential, which is governed by the conduction band edge energy.[7–9] Thus, the classic electrochemical method for introducing reaction selectivity when using a metal electrode, adjusting the operating potential, is not available. While one can consider electrode materials that produce electrons at other potentials, through generation of hot electrons or introduction of electrochemically active surfaces states, for example, these approaches tend to lead to enhanced electron-hole recombination and, accordingly, low charge transfer efficiencies.[7–9]

To circumvent this conundrum we consider a strategy that utilizes a semiconductor that is efficient at the requiste optically induced charge separation processes, but is inept at interfacial charge transfer.

An efficient and selective electrocatalyst is then added to the surface of the semiconductor. In other words, without the added electrocatalyst, the semiconductor-electrolyte interface could be described as "ideally noncatalytic." In this scheme, the semiconductor surface must be incapable of facilitating electrochemical reactions, since any direct semiconductor-based processes will lead to a lack of selectivity for the chemistry of interest. We coin this concept "catalytic mismatch," which is dependent upon strategic selection of the semiconductor component. By analogy, the semiconductor in such a catalytically mismatched system can be compared to the solid support material used in traditional electrocatalysis. Solid supports are selected based on their high conductivity matched with chemical non-reactivity[10]; in a catalytically mismatched system, the semiconductor is a functional solid support whose non-reactivity is paired with prime optical energy conversion capabilities. While the addition of an interfacial electrocatalyst to the surface of a photoelectrode is fairly routine, the selection of a semiconductor that is completely non-electrocatalytic provides the novel aspect of the proposal put forth here.

Support for this concept comes from a recent publication from our research group reporting on photocatalytic H_2 evolution using the chalcopyrite semiconductor series $Ag_xCu_{1-x}Ga_yIn_{1-y}S_2$.[11] In that case, Cu-rich systems were shown to be inherently noncatalytic for H_2 evolution, in direct contrast to the Ag-rich analogs. Upon addition of Pt, a well-known H_2 evolution electrocatalyst, to the surface of the Cu-rich samples, a photocatalytic H_2 evolution pathway was activated. No effect was observed when Pt was added to the already-active Ag-rich species. Here, we provide the formative case study of catalytic mismatching used to achieve a product-selective, CO_2-reducing photoelectrode, featuring an inherently noncatalytic semiconductor, *p*-type $CuInSe_2$, paired with the electrocatalyst Ni_3Al.[12]

$CuInSe_2$ has a direct bandgap of 0.92 eV.. We previously studied $CuInSe_2$ as a photocathode for water reduction; in these experiments, $CuInSe_2$ proved to be kinetically sluggish and prone to photoinduced reductive decomposition under certain environmental conditions.[13] However, the optical formation of electron-hole pairs was an efficient process (i.e., > 90% Faradaic efficiency) at energies just slightly larger than the band gap energy.[13] Now we consider the electrochemically more-challenging reaction of CO_2 reduction at this interface. While the conduction band edge of the material is energetically well-situated for this process,[14] the reaction dynamics are expected to make generation of carbon-containing products

insignificant. To convert this electrode interface into an electrochemically interesting material, we have supplied the semiconductor surface with Ni_3Al and TiO_2, modifying agents which suppress photodecomposition and turn on CO_2 reduction activity. This composite photoelectrochemical system, hereafter referred to as $CuInSe_2/Ni_3Al+TiO_2$, produces methanol at a Faradaic efficiency 25 times greater than that

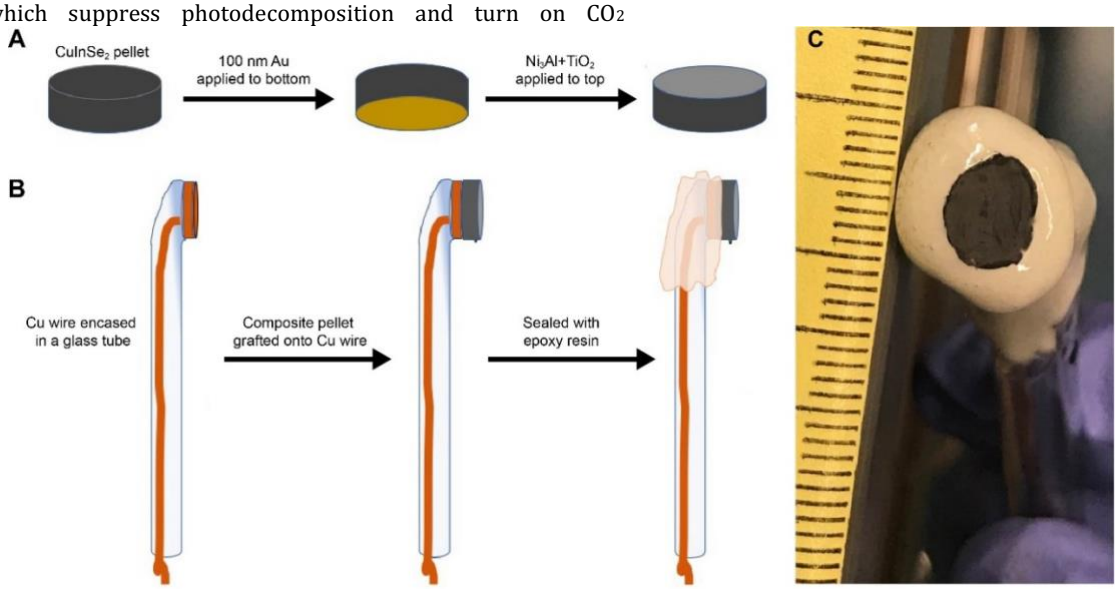

Figure 1. Fabrication of the $CuInSe_2/Ni_3Al+TiO_2$ electrode configuration. (A) $CuInSe_2$ pellet preparation involved sputtering a layer of Au on one side and painting an aqueous slurry of $Ni_3Al+TiO_2$ on the other. (B) The pellet was connected via the back Au contact to a Cu wire and threaded through a glass casing; the composite electrode was sealed with insulating epoxy. (C) The resulting electrodes exhibited average geometric surface areas of 0.25 cm^2.

achieved using the purely electrochemical Ni_3Al system,[12] while simultaneously lowering the operating potential requirement by 600 mV when compared to the same catalyst applied to a glassy carbon surface.

Preliminary electrochemical testing performed using bare $CuInSe_2$ electrodes resulted in semiconductor degradation, regardless of electrolyte pH.[13] As noted in previous studies, this behavior is characteristic of Cu reduction (i.e., from the semiconductor, Cu^+ to Cu^0).[13,15] Addition of a TiO_2 surface layer, a known protective agent,[16,17] failed to prevent corrosion due to introduction of a Schottky barrier. More information on preliminary electrode preparation trials can be found in Supporting Text S1. We note here in passing that Yuan *et al.* claims to have observed that the related *p*-type chalcopyrite $CuInS_2$ photoelectrochemically reduces CO_2 in the presence of dissolved pyridine[18,19]; however, these studies lacked a critical $^{13}CO_2$ labeling experiment and could not be reproduced in our laboratory.

Since initial results suggested that $CuInSe_2$ was incapable of facilitating CO_2 reduction on its own, supporting our initial hypothesis, it served as an ideal semiconductor material with which to pair an active CO_2-reducing electrocatalyst, thereby testing the concept of catalytic mismatching. Given its ability to generate highly reduced products from CO_2,[12] the intermetallic Ni_3Al was selected as the electrocatalyst. Alternative literature systems that combine photoabsorbers and CO_2-reducing electrocatalysts have been limited to photo- or photoelectrochemical generation of formate or CO, two-electron-reduced species, as the dominant products and, critically, have not been designed specifically based on the principle of catalytic mismatching.[20–22]

To achieve a uniform layer of Ni_3Al on the semiconductor surface, the intermetallic powder was mixed with an equal quantity of TiO_2 (by volume) in water and coated onto the electrode, as illustrated in Figure 1. Materials characterization was conducted on the final $CuInSe_2/Ni_3Al+TiO_2$ composite to further support the validity of the established electrode fabrication method.

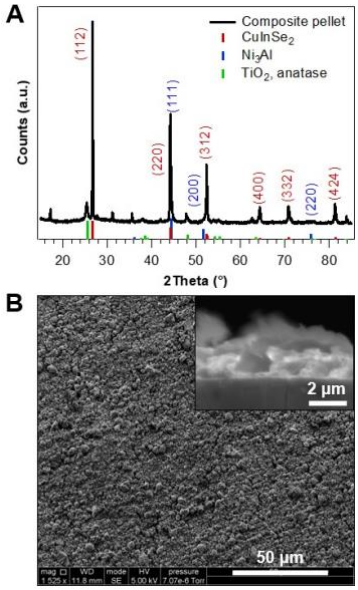

Figure 2. Materials characterization of $CuInSe_2/Ni_3Al+TiO_2$. (A) XRD pattern of the as-synthesized composite pellet. Reference peaks correspond to PDF patterns as follows: $CuInSe_2$ (00-063-0126, indexed in red); Ni_3Al (01-071-5883, indexed in blue); anatase TiO_2 (01-070-6826). (B) SEM before electrochemical experimentation, confirming both surface homogeneity and morphological stability. Based on analysis of the pellet cross-section (inset), the thickness of the $Ni_3Al+TiO_2$ layer is 2–3 µm.

X-ray diffraction (XRD; Figure 2A) performed on the as-fabricated electrode confirmed the presence of $CuInSe_2$, Ni_3Al,

and TiO_2, with $CuInSe_2$ appropriately dominating the bulk composition. As seen in the scanning electron microscopy (SEM) image in Figure 2B, the intermetallic and TiO_2 were uniformly distributed across the surface of the electrode. This coating exhibited a thickness of ~2–3 μm, thereby providing substantial coverage of the semiconductor surface. Further material characterization was performed using energy-dispersive X-ray spectroscopy (EDX) and X-ray photoelectron spectroscopy (XPS) (Figures S1, S2).

To assess the photoelectrochemical CO_2 reduction activity of the $CuInSe_2/Ni_3Al+TiO_2$ composite electrode, linear sweep voltammetry (LSV) was performed. As shown in Figure 3A, current enhancement occurred around –0.4 V vs. Ag/AgCl under CO_2 saturation compared to Ar, suggesting the onset of CO_2 reduction. The presence of a photocurrent was also revealed using chopped-light LSVs obtained in a CO_2-saturated environment (Figure 3B). This confirmed that the incident light successfully penetrated beyond the 2–3 μm layer of $Ni_3Al+TiO_2$, in agreement with the absorbance measurements and subsequent absorption depth calculations previously performed.[13]

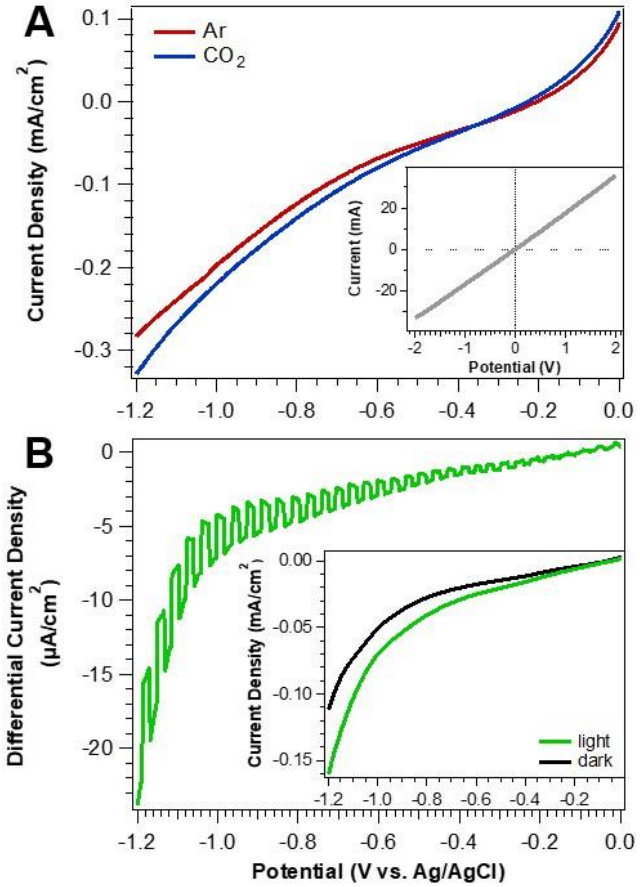

Figure 3. LSV characterization of $CuInSe_2/Ni_3Al+TiO_2$. (A) Following confirmation of ohmic contact (inset), LSVs obtained under illumination and either Ar (red) or CO_2 (blue) saturation suggest that the onset of CO_2 reduction occurs around –0.4 V vs. Ag/AgCl. (B) The CO_2-saturated, chopped-light LSV (where dark current is subtracted to portray differential current density) and standard LSVs collected under dark and light conditions (inset) indicate that a photocurrent is present despite the uniform metal catalyst coating on the surface. Data were collected using 0.1 M $KHCO_3$ electrolyte (pH 7), 25 mV/s scan rate, and a 150 W Xe arc lamp at 200 mW/cm_2 using an IR filter.

This result is further supported by LSVs obtained separately under light and dark conditions (Figure 3B, inset), which show a noticeable difference in current density. Based on the i-V curve, the flat band potential of this composite electrode is near –0.1 V vs. Ag/AgCl, consistent with the limiting potential found in open-circuit photovoltage measurements.

Methanol was the primary CO_2 reduction product achieved, as confirmed using a mixture of $^{13}CO_2/^{12}CO_2$ starting material (Figure S3) and analyzing the appearance of ^{13}C methanol using ^1H-nmr. Integration of the nmr data indicates a ratio of 70:30 ^{13}C to ^{12}C in the product – a ratio consistent with the ratio of $^{13}CO_2/^{12}CO_2$ employed, and unambiguously demonstrating that the observed methanol derives from CO_2. Subsequently, control experiments were undertaken to ensure that all components of the composite photoelectrode are required to achieve methanol production. Indeed, photoelectrolyses conducted using only TiO_2 or $Ni_3Al+TiO_2$ (i.e., without $CuInSe_2$) resulted in the generation of only H_2 and trace amounts of formate. Following this confirmation, preliminary testing with the complete $CuInSe_2/Ni_3Al+TiO_2$ electrode revealed that stable current densities around –0.1 mA/cm_2 could be achieved at –1.0 V vs. Ag/AgCl during a 16-h period (Figure 4A). During this time, CO_2 reduction competed with H_2 evolution—a frequent challenge[23]—and CO was not evident in the gas-phase (Figure S4). These results confirmed charge and mass balance, so subsequent photoelectrolysis experiments were conducted under a constant flow of CO_2 (i.e., not sampling the gas phase).

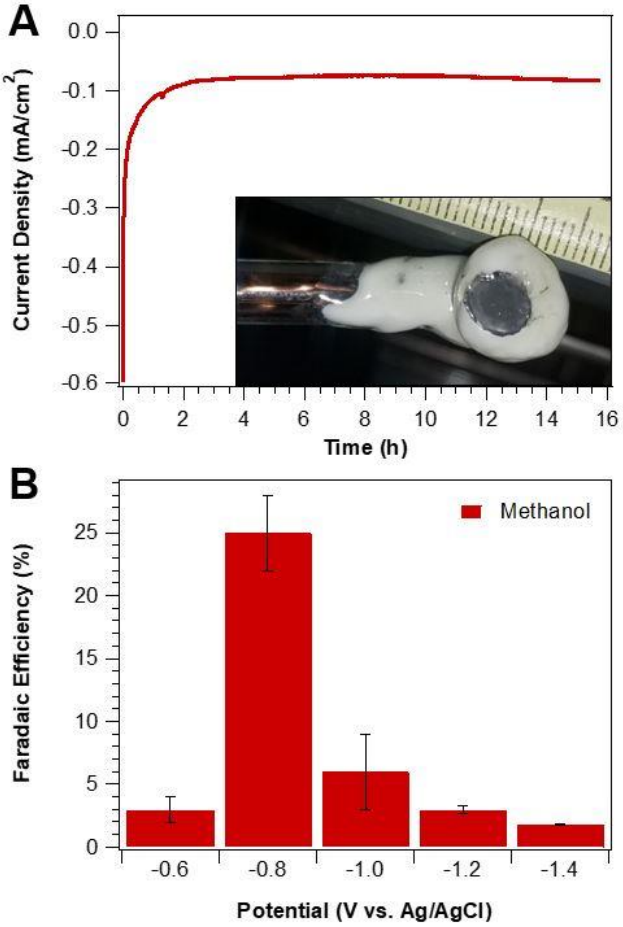

Figure 4. Performance of the $CuInSe_2/Ni_3Al+TiO_2$ composite electrode during bulk photoelectrolysis. (A) At –1.0 V vs. Ag/AgCl, stable photoelectrochemical current could be

achieved for nearly 16 h, resulting in no physical degradation of the electrode (inset). The initial decrease in current at t = 0 h is attributed to the reduction of surface oxides. (B) Faradaic efficiencies for photoelectrochemical CO_2 reduction to methanol are reported at various operating potentials, where a maximum value of 25 ± 3% was recorded at –0.8 V vs. Ag/AgCl. Experiments were conducted in 0.1 M $KHCO_3$ (pH 7) using a 150 W Xe arc lamp at 200 mW/cm^2.

Remaining bulk photoelectrolysis experiments were performed using 0.1 M $KHCO_3$ electrolyte, a 200 mW/cm^2 light source, and operating potentials ranging from –0.6 to –1.4 V vs. Ag/AgCl. The results of these experiments are shown in Figure 4B, which plots the Faradaic efficiencies for methanol achieved using this composite electrode. At most operating potentials, methanol Faradaic efficiencies ranged from 2–6%. However, the CO_2 reduction activity of this system is highly potential-dependent, signifying a reintroduction of potential-based control compared to the expected behavior of an ideal semiconductor-electrolyte system. This is evidenced by a maximum Faradaic efficiency of 25% achieved at –0.8 V vs. Ag/AgCl, representing nearly five times higher methanol production than the second highest Faradaic efficiency. To the best of our knowledge, this is the first example of combining a chalcopyrite material with an electrocatalyst to generate methanol in photoelectrochemical CO_2 reduction.

Our initial report of the entirely electrochemical Ni_3Al/glassy carbon electrocatalyst indicated that Faradaic efficiencies for methanol peaked at 1.0% using an operating potential of –1.38 V vs. Ag/AgCl, and small quantities of formate were produced.[12] The $CuInSe_2$/Ni_3Al+TiO_2 composite electrode studied here also generated trace amounts of formate. The absence of CO, which, in the glassy carbon study, was recorded at ~30% Faradaic efficiency and observed to be an intermediate en route to products like methanol, may have been generated and efficiently converted to methanol at the $CuInSe_2$/Ni_3Al+TiO_2 surface. In fact, use of a CO feedstock in the composite photoelectrochemical system in place of CO_2 did yield methanol, albeit at a lower Faradaic efficiency (i.e., ~10% when operating at –0.8 V vs. Ag/AgCl). Nonetheless, the methanol Faradaic efficiencies achieved photoelectrochemically using $CuInSe_2$/Ni_3Al+TiO_2 exceed those achieved by the electrochemical Ni_3Al analog at all potentials studied. However, it should be noted that a significant dark current was observed in this study, as seen in Figure S5. Under this condition, it is likely that the Ni_3Al within the $CuInSe_2$/Ni_3Al+TiO_2 composite behaves strictly as an electrocatalyst, whose slow electron transfer kinetics (i.e., low current density compared to the previously reported Ni_3Al/glassy carbon electrochemical system) favor generation of the one-carbon product methanol as opposed to the other liquid-phase, multi-carbon products achieved by Ni_3Al/glassy carbon. Efforts to understand the source of this dark current, as well as the nature of the catalytic layer and the catalyst-semiconductor interface, are the focus of ongoing studies. In any case, post-electrolysis materials characterization revealed that the composite electrode remained intact following photoelectrochemical experimentation (Figures S6–S9).

The $CuInSe_2$/Ni_3Al+TiO_2 composite electrode presented in this work represents the formative case study of catalytic mismatching by combining a CIGS photoabsorber with a CO_2-reducing catalyst to achieve photoelectrochemical reduction of CO_2 to methanol, with Faradaic efficiencies reaching up to 25%. In doing so, this system affirms the utility of a novel photoelectrode design strategy—combining a catalytically inactive yet optically proficient semiconductor with a known electrocatalyst—in facilitating selective CO_2 reduction. Nonetheless, opportunities for improving CO_2 reduction efficiency exist, creating a springboard for future research into this photoelectrocatalytic system and others that could be designed using a similar strategy. In fact, the results of this study leave much room for exploring additional combinations of CIGS photoabsorbers, as well as other electrochemically unreactive semiconductors, with heterogeneous electrocatalysts to unlock new photoelectrochemical CO_2 reduction activity, though alternative catalytic processes should also be possible. As such, the composite $CuInSe_2$/Ni_3Al+TiO_2 system motivates the use and exemplifies the importance of catalytic mismatching as a strategy for future photoelectrochemical design.

ASSOCIATED CONTENT

Supporting Information

The Supporting Information is available free of charge on the ACS Publications website.

Experimental methods, electrode configurations, additional materials characterization, labeled product analysis, dark electrolysis results

AUTHOR INFORMATION

Corresponding Author

*Email: bocarsly@princeton.edu

ORCID

Aubrey R. Paris: 0000-0002-9525-7129
Andrew B. Bocarsly: 0000-0003-3718-0933

Author Contributions

BMF and DABP conducted most electrochemical and photoelectrochemical experiments. ARP performed isotopic labeling and CO feedstock experiments. ARP and JJF collected materials characterization data and oversaw project development and progress. All authors contributed to data analysis.

Notes

The authors declare no competing financial interests.

ACKNOWLEDGMENTS

The authors thank the National Science Foundation for financially supporting this work under Grant CHE-1800400. B.M.F. and D.A.B.-P. acknowledge the Leach Summer Scholars Program, the Summer Undergraduate Research Program for Diversity in Chemistry at Princeton University, and J.K.R. A.R.P. and J.J.F. acknowledge support by the National Science Foundation Graduate Research Fellowship Program under Grant Nos. DGE-1148900 and DGE-1656466, respectively. The authors acknowledge the use of Princeton's Imaging and Analysis Center, which is partially supported by the Princeton Center for Complex Materials, a National Science Foundation MRSEC program (DMR-1420541). Any opinions, findings, and conclusions or recommendations expressed in this material are those of the authors and do not necessarily reflect the views of the National Science Foundation.

REFERENCES

(1) O'Regan, B.; Gratzel, M. A Low-Cost, High-Efficiency Solar Cell Based on Dye-Sensitized Colloidal TiO_2 Films. *Nature* 1991, *353*, 737–740.

(2) Maeda, K.; Takata, T.; Hara, M.; Saito, N.; Inoue, Y.; Kobayashi, H.; Domen, K. GaN:ZnO Solid Solution as a Photocatalyst for Visible-Light-Driven Overall Water Splitting. *Journal of the American Chemical Society* **2005**, *127* (23), 8286–8287. https://doi.org/10.1021/ja0518777.

(3) Maeda, K.; Domen, K. Photocatalytic Water Splitting: Recent Progress and Future Challenges. *The Journal of Physical Chemistry Letters* **2010**, *1* (18), 2655–2661. https://doi.org/10.1021/jz1007966.

(4) Maeda, K. Photocatalytic Water Splitting Using Semiconductor Particles: History and Recent Developments. *Journal of Photochemistry and Photobiology C: Photochemistry Reviews* **2011**, *12* (4), 237–268.

(5) Hisatomi, T.; Kubota, J.; Domen, K. Recent Advances in Semiconductors for Photocatalytic and Photoelectrochemical Water Splitting. *Chem. Soc. Rev.* **2014**, *43* (22), 7520–7535. https://doi.org/10.1039/C3CS60378D.

(6) White, J. L.; Baruch, M. F.; Pander III, J. E.; Hu, Y.; Fortmeyer, I. C.; Park, J. E.; Zhang, T.; Liao, K.; Gu, J.; Yan, Y.; Shaw, T.W.: Abelev, E.; Bocarsly, A.B.; . Light-Driven Heterogeneous Reduction of Carbon Dioxide: Photocatalysts and Photoelectrodes. *Chemical Reviews* **2015**, *115* (23), 12888–12935. https://doi.org/10.1021/acs.chemrev.5b00370.

(7) Sze, S. M.; Ng, K. K. *Physics of Semiconductor Devices*, 3rd ed.; John Wiley & Sons, Inc.: Hoboken, New Jersey, 2007.

(8) Neamen, D. A. *Semiconductor Physics and Devices: Basic Principles*, 4th ed.; McGraw-Hill: New York, New York, 2011.

(9) Chen, Z.; Dinh, H. N.; Miller, E. *Photoelectrochemical Water Splitting: Standards, Experimental Methods, and Protocols*; Springer: New York, New York, 2013.

(10) Yang, N.; Waldvogel, S. R.; Jiang, X. Electrochemistry of Carbon Dioxide on Carbon Electrodes. *ACS Applied Materials & Interfaces* **2016**, *8* (42), 28357–28371. https://doi.org/10.1021/acsami.5b09825.

(11) Ni, D.; Kuo, H.-Y.; Park, J. E.; Lee, T. S.; Sloman, S.-R. I.; Cava, R. J.; Bocarsly, A. B. Improved H_2 Evolution in Quaternary SCIGS Chalcopyrite Semiconductors. *The Journal of Physical Chemistry C* **2018**, *122* (43), 24512–24519. https://doi.org/10.1021/acs.jpcc.8b05389.

(12) Paris, A. R.; Bocarsly, A. B. Ni–Al Films on Glassy Carbon Electrodes Generate an Array of Oxygenated Organics from CO_2. *ACS Catalysis* **2017**, *7* (10), 6815–6820. https://doi.org/10.1021/acscatal.7b02146.

(13) Frick, J. J.; Cava, R. J.; Bocarsly, A. B. Chalcopyrite $CuIn(S_{1-x}Se_x)_2$ for Photoelectrocatalytic H_2 Evolution: Unraveling the Energetics and Complex Kinetics of Photogenerated Charge Transfer in the Semiconductor Bulk. *Chemistry of Materials* **2018**, *30* (13), 4422–4431. https://doi.org/10.1021/acs.chemmater.8b01827.

(14) Frick, J. J.; Kushwaha, S. K.; Cava, R. J.; Bocarsly, A. B. Characterization of Primary Carrier Transport Properties of the Light-Harvesting Chalcopyrite Semiconductors $CuIn(S_{1-x}Se_x)_2$. *The Journal of Physical Chemistry C* **2017**, *121* (32), 17046–17052. https://doi.org/10.1021/acs.jpcc.7b03152.

(15) Gu, J.; Yan, Y.; Krizan, J. W.; Gibson, Q. D.; Detweiler, Z. M.; Cava, R. J.; Bocarsly, A. B. *P*-Type $CuRhO_2$ as a Self-Healing Photoelectrode for Water Reduction under Visible Light. *Journal of the American Chemical Society* **2014**, *136* (3), 830–833. https://doi.org/10.1021/ja408876k.

(16) Jiao Zhao, J.; Minegishi, T.; Zhang, L.; Zhong, M.; Gunawan; Nakabayashi, M.; Ma, G.; Hisatomi, T.; Katayama, M.; Ikeda, S.; Shibata, N.; Yamada, T.; Domen, K.; Enhancement of Solar Hydrogen Evolution from Water by Surface Modification with CdS and TiO_2 on Porous $CuInS_2$ Photocathodes Prepared by an Electrodeposition-Sulfurization Method. *Angewandte Chemie International Edition* **2014**, *53* (44), 11808–11812. https://doi.org/10.1002/anie.201406483.

(17) Luo, J.; Tilley, S. D.; Steier, L.; Schreier, M.; Mayer, M. T.; Fan, H. J.; Grätzel, M. Solution Transformation of Cu_2O into $CuInS_2$ for Solar Water Splitting. *Nano Letters* **2015**, *15* (2), 1395–1402. https://doi.org/10.1021/nl504746b.

(18) Yuan, J.; Hao, C. Solar-Driven Photoelectrochemical Reduction of Carbon Dioxide to Methanol at $CuInS_2$ Thin Film Photocathode. *Solar Energy Materials and Solar Cells* **2013**, *108*, 170–174. https://doi.org/10.1016/j.solmat.2012.09.024.

(19) Yuan, J.; Wang, P.; Hao, C.; Yu, G. Photoelectrochemical Reduction of Carbon Dioxide at CuInS 2 /Graphene Hybrid Thin Film Electrode. *Electrochimica Acta* **2016**, *193*, 1–6. https://doi.org/10.1016/j.electacta.2016.02.037.

(20) Choi, S. K.; Kang, U.; Lee, S.; Ham, D. J.; Ji, S. M.; Park, H. Sn-Coupled p-Si Nanowire Arrays for Solar Formate Production from CO_2. *Advanced Energy Materials* **2014**, *4* (11), 1301614. https://doi.org/10.1002/aenm.201301614.

(21) Shen, Q.; Chen, Z.; Huang, X.; Liu, M.; Zhao, G. High-Yield and Selective Photoelectrocatalytic Reduction of CO_2 to Formate by Metallic Copper Decorated Co_3O_4 Nanotube Arrays. *Environmental Science & Technology* **2015**, *49* (9), 5828–5835. https://doi.org/10.1021/acs.est.5b00066.

(22) Suzuki, T. M.; Yoshino, S.; Takayama, T.; Iwase, A.; Kudo, A.; Morikawa, T. Z-Schematic and Visible-Light-Driven CO_2 Reduction Using H_2O as an Electron Donor by a Particulate Mixture of a Ru-Complex/$(CuGa)_{1-x}Zn_{2x}S_2$ Hybrid Catalyst, $BiVO_4$ and an Electron Mediator. *Chemical Communications* **2018**, *54* (72), 10199–10202. https://doi.org/10.1039/C8CC05505J.

(23) Ooka, H.; Figueiredo, M. C.; Koper, M. T. M. Competition between Hydrogen Evolution and Carbon Dioxide Reduction on Copper Electrodes in Mildly Acidic Media. *Langmuir* **2017**, *33* (37), 9307–9313. https://doi.org/10.1021/acs.langmuir.7b00696.

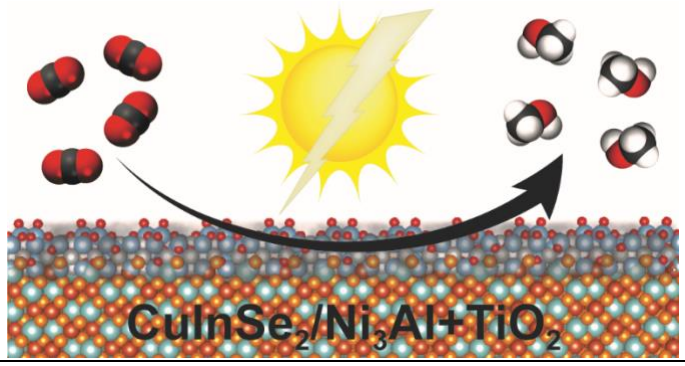
$CuInSe_2/Ni_3Al+TiO_2$